

One-dimensional modelling of individual waves and wave-induced longshore currents in the surf zone

L.C. van Rijn^{a,b}, K.M. Wijnberg^a

^a Dept. Phys. Geography, Univ. of Utrecht, P.O. Box. 80115, 3508 TC Utrecht, Netherlands

^b Delft Hydraulics, P.O. Box 152, 8300 AD Emmeloord, Netherlands

Received 22 March 1995; accepted 9 February 1996

Abstract

A probabilistic model (WAVIS-model) was developed to describe the propagation and transformation of individual waves (wave by wave approach). The individual waves shoal until an empirical criterion for breaking is satisfied. Wave height decay after breaking is modelled by using an energy dissipation method. Wave-induced set-up and set-down and breaking-associated longshore currents are also modelled. Laboratory and field data were used to calibrate and verify the model. The model was calibrated by adjusting the wave breaking coefficient (as a function of local wave steepness and bottom slope) to obtain optimum agreement between measured and computed wave height. Four tests carried out in the large Delta flume of Delft Hydraulics were considered. Generally, the measured $H_{1/3}$ -wave heights are reasonably well represented by the model in all zones from deep water to the shallow surf zone. The fraction of breaking waves was reasonably well represented by the model in the upsloping zones of the bottom profile. Verification of the model results with respect to wave-induced longshore current velocities was not extensive, because of a lack of data. In case of a barred profile the measured longshore velocities showed a relatively uniform distribution in the (trough) zone between the bar crest and the shoreline, which could to some extent be modelled by including space-averaging of the radiation force gradient, horizontal mixing and longshore water surface gradients related to variations in set-up. In case of a monotonically upsloping profile the cross-shore distribution of the longshore current velocities is reasonably well represented.

1. Introduction

Two types of models are commonly used to describe the propagation and transformation of waves over (barred) nearshore profiles along uniform beaches: parametric models and probabilistic models.

The parametric models are based on the wave-energy or wave-action balance in terms of the root mean square wave height (H_{rms}) and the peak period to represent the (single peaked) wave spectrum. Special distributions are used to represent the height of breaking waves. The energy dissipation of breaking waves is modelled in analogy with the energy dissipation of a propagating bore (Le Méhauté, 1962). A popular method is that proposed by Battjes and Janssen (1978) which is based on a Rayleigh-distribution of wave heights, truncated at the breaker (maximum) wave height. Functions are specified to determine the maximum wave height and the percentage of breaking waves. Parametric wave models are used by Battjes and Janssen (1978), Thornton and Guza (1983), Stive and Dingemans (1984), Roelvink (1993), Southgate and Nairn (1993) and by Kamphuis (1994).

The probabilistic models are based on propagation and transformation of individual waves (wave by wave approach). The probability density function of the wave height in deep water is schematized into a discrete series of wave height classes and corresponding periods. Each wave height class is assumed to propagate shoreward independently of the other classes by solving the wave-energy balance separately. The individual waves shoal until an empirical criterion for breaking is satisfied. Wave height decay after breaking is modeled by energy dissipation methods or by exponential adjustment to a stable wave height. At any location the wave statistics such as the root mean square wave height (H_{rms}) or the significant wave height ($H_{1/3}$) are calculated from the predicted individual wave heights. Probabilistic models have been used by Mase and Iwagaki (1982), Mizuguchi (1982), Dally et al. (1985), Dally and Dean (1986) and Dally (1992). Breaking-associated longshore currents were not considered by these models.

Accurate modelling of sand transport in the nearshore zone and surfzone with bars requires rather accurate representation of the processes of shoaling, breaking and reforming of especially the higher waves because of the strongly non-linear dependency of sand transport on wave height.

According to the authors, the probabilistic models offer a promising solution for accurate determination of sand transport rates across barred nearshore profiles.

In this paper a probabilistic model is presented (WAVIS-model; WAVes In Surfzone) that describes the transformation of shoreward propagating irregular waves and the associated longshore currents due to wave breaking. The model is calibrated and verified using laboratory and field data, focussing on barred cross-shore profiles.

2. Model description

Oblique-incident and normal-incident waves are assumed to propagate unidirectionally (without wave reflection) toward a straight beach with parallel depth contours.

The wave propagation and transformation processes incorporated in the model are: refraction, shoaling by depth variations and (Doppler shifting) by depth-averaged longshore currents and energy dissipation by bottom friction and breaking.

The processes of shoaling and breaking are assumed to be unaffected by wave-wave interaction and wave overtaking. Wave reflection is not modelled. Long wave effects (interaction with surf beat) are not considered. Variation of the mean water surface level

(set up, set down) related to radiation stress variations is included. Wave conditions are specified at the offshore boundary as a series of discrete wave height classes and corresponding periods.

2.1. Wave action balance

The wave action balance reads as:

$$\frac{d}{dx} \left(\frac{EC_{g,r} \cos \theta + u}{\omega_r} \right) + \frac{D_{bf} + D_{br}}{\omega_r} = 0 \quad (1)$$

in which $E = \rho g H^2 / 8$ = wave energy per unit area; $C_{g,r} = n C_r$ = relative wave group velocity; $\omega_r = 2\pi / T_r$ = relative wave angular frequency; $\theta = \arcsin[(C_r / C_{r,0}) \sin \theta_0]$ = angle of wave ray and x -axis normal to coast; D_{bf} = energy dissipation per unit area by bottom friction; D_{br} = energy dissipation per unit area by breaking; H = wave height; $T_r = T / [1 - (T|\vec{v}| \cos \phi / L)]$ = relative wave period; ρ = fluid density; g = acceleration of gravity; \vec{v} = depth-averaged velocity vector; u = depth-averaged current velocity component in x -direction; ϕ = angle between wave propagation direction and current direction; $C_r = L / T_r$ = relative wave propagation velocity; L = wave length; T = absolute period; $n = 0.5[1 + 2kh / \sinh(2kh)]$ = coefficient; $k = 2\pi / L$ = wave number; x = coordinate normal to shore (positive in onshore direction).

The wave length is defined by the dispersion relation including the current refraction (Doppler shifting) effect:

$$\left[\frac{L}{T} - |\vec{v}| \cos \phi \right]^2 = \frac{gL}{2\pi} \tanh \left(\frac{2\pi h}{L} \right) \quad (2)$$

in which h = local water depth (to still water surface).

Energy dissipation by bottom friction is described by (Putnam and Johnson, 1949):

$$D_{bf} = \frac{\rho f_w}{6\pi} \left[\frac{\omega_r H}{\sinh(2\pi h / L)} \right]^3 \quad (3)$$

The friction coefficient (f_w) in the hydraulically rough regime can be expressed as:

$$f_w = \exp \left[-6 + 5.2 \left(\hat{A}_s / k_{s,w} \right)^{-0.19} \right], \quad f_{w,max} = 0.3 \quad (4)$$

in which \hat{A}_s = peak value of near-bed orbital excursion; $k_{s,w}$ = effective bed roughness height. The effect of cross-shore and longshore currents on the near-bed wave motion is negligible small (Van Rijn, 1993). Hence, the wave-related bottom friction in the coastal zone can be represented with sufficient accuracy by Eq. (4).

Various researchers (Mase and Iwagaki, 1982; Mizuguchi, 1982; Dally, 1992; Kamphuis, 1994) have observed that the use of linear wave theory leads to an underestimation of the height of the longer waves in the outer surf zone, especially for low deep-water wave steepness. The shoaling of these waves is much better described by cnoidal wave theory. Relatively simple expressions for normal incident waves are given by Shuto (1974). The application of Cnoidal wave theory for obliquely incident

waves in the presence of currents is rather complicated and not yet solved. Further studies are required.

2.2. Wave breaking

Waves are assumed to break if the local wave height (H) found in the model is larger than the local maximum possible wave height (H_{\max}) associated with breaking.

The energy dissipation in a breaking wave can be described by an expression based on the analogy between dissipation of energy in a breaking wave and in a bore (Battjes and Janssen, 1978; Roelvink, 1993), yielding:

$$D_{\text{br}} = 0.25 \alpha_1 \rho g \frac{H^2}{T_r} \quad (5)$$

with α_1 = calibration coefficient (≈ 1); ρ = fluid density.

In the present model a modified expression, yielding a gradual transition to a zero dissipation for $H = H_{\max}$, is used:

$$D_{\text{br}} = 0.25 \alpha_2 \rho g \left(\frac{H^2 - H_{\max}^2}{T_r} \right) \quad \text{if } H > H_{\max} \quad (6)$$

with α_2 = calibration coefficient;

$$H_{\max} = \text{minimum} [\gamma h, 0.14 L \tanh(kh)] \quad (7)$$

Eq. (7) implies that the H_{\max} -value at any location is determined by wave breaking either on depth ($H_{\max} = \gamma h$) or on steepness ($H_{\max} = 0.14 L \tanh(kh)$). The fraction of breaking waves at a certain location is obtained by summing the percentages of occurrence of the wave height classes that are breaking ($H > H_{\max}$) at that location.

The α_2 -factor is 1.5, and was found by calibration using laboratory and field data. The breaking coefficient γ is assumed to depend on the ratio of the local bottom slope ($\tan\beta$) and the local wave steepness (H/L). The local bottom slope is taken to be the average bottom slope of the profile over a distance of β times the local wave length seaward of the local coordinate. In most computations a β -factor of 0.5 was used. The influence of the β -factor is discussed in section 3 on calibration. A negative bottom slope on the landward side of a sand bar is set to a zero slope value.

For breaking of regular waves the γ -factor of Weggel (1972) is commonly used (Dally, 1992; Southgate and Nairn, 1993). In irregular wave conditions the formula of Weggel cannot be used because it yields unrealistically large γ -values between 0.78 and 1.5 depending on the bottom slope and wave steepness parameters. Nelson (1983) and Horikawa and Kuo (1966) have shown that the maximum wave height over a horizontal bottom ($\tan\beta = 0$) is about 0.4 to 0.5 of the water depth. Sato et al. (1990) have found that individual waves in a random wave field break at smaller heights than in a monochromatic wave field due to the presence of long wave components generated in a random wave field. Maximum γ -factors were found to be about 1.1 for a bottom slope of 1:10.

In the WAVIS model the γ -factor varies between 0.45 and 1 depending on the ratio of $\tan\beta$ and H/L , as presented in Fig. 1. This curve was obtained by calibration.

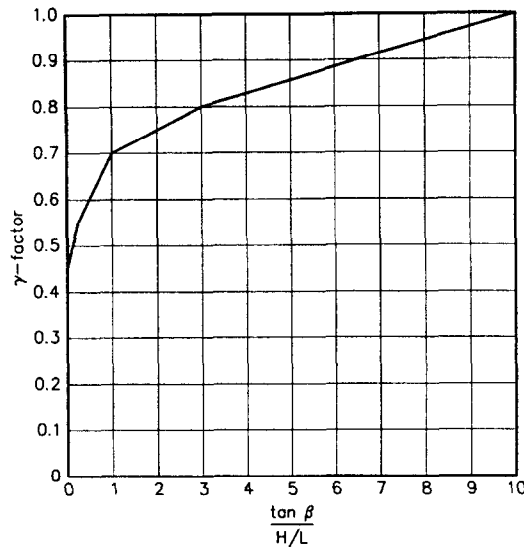


Fig. 1. Breaking coefficient.

The present method is different from the method used by Dally (1992). In his model individual waves shoal until the condition for incipient breaking developed by Weggel (1972) is satisfied. Wave height decay after breaking is determined by exponential adjustment to a stable wave height which is equal to about 0.4 of the local water depth (h) for all conditions. In this schematization (based on the experimental results of Horikawa and Kuo, 1966) a difference is being made between the initiation of breaking and the cessation of breaking; the former occurring at a higher value of wave height to depth ratio. In the experiments of Horikawa and Kuo the bottom consisted of a steep slope section of 1 to 5 followed by a less steep (maximum 1 to 20) or horizontal section. The incident waves were forced to break at the end of the steep slope section and the wave height decay after breaking was monitored. The results of Horikawa and Kuo were interpreted by Dally et al. (1985) in terms of a wave height stabilizing at a constant value (cessation of breaking) lower than that related to the initiation of breaking. It should be realized, however, that the initiation of breaking was forced to occur at the end of the steep slope section (1 to 5), whereas the cessation of breaking took place on a gentle sloping (or horizontal) bed. Analysis of the data of Horikawa and Kuo clearly shows that the stable wave height (after breaking) depends on the bottom slope. It increases from 0.4 h for a horizontal bottom to about 0.5 h for a slope of 1 to 65; to 0.65 h for a slope of 1 to 30 and to 0.8 h for a slope of 1 to 20 (see Fig. 9 of Horikawa and Kuo, 1966). The results of Horikawa and Kuo can be reasonably well represented by the present model (see Fig. 1). Generally, the measured values of Horikawa and Kuo are about 10% to 15% smaller than those given in Fig. 1. Hence, the present analysis (based on verification over a wide range of conditions) does not show the need for a separation between the initiation of breaking and the cessation of breaking, as long as the breaking coefficient (and thus H_{\max}) is modelled as a function of bottom slope and wave steepness.

2.3. Set-up and set-down of the mean water surface level

The wave-induced set-up and set-down are determined from the time-averaged momentum balance neglecting inertial effects and bed-shear stress, which reads as follows:

$$\frac{dS_{xx}}{dx} + \rho g(h+s) \frac{ds}{dx} - \tau_{sf} = 0 \quad (8)$$

in which S_{xx} = onshore radiation force (herein the terminology force rather than stress is preferred because S_{xx} represents a force per unit length); s = mean water level change (set-up/set-down) and $\tau_{sf} = \tau_{wind} + \tau_{sr}$ = shear stress at water surface to account for the wind effect (τ_{wind}) and the breaking roller effect (τ_{sr}).

The wind-shear stress can be represented as $\tau_{wind,x} = \rho_a f_a w_{10} |w_{10,x}|$ with ρ_a = air density (= 1.25 kg/m³), f_a = friction coefficient (= 0.001 to 0.002) and w_{10} = magnitude of the wind velocity vector at 10 m above the surface, $w_{10,x}$ = wind velocity component in x -direction.

The breaker roller effect can also be represented by a shear stress acting at the wave trough level. The τ_{sr} -parameter is herein modelled as $\tau_{sr} = \alpha_{sr} \rho f_s c^2$ with $c^2 = g(h+s)$, f_s = friction coefficient (= 0.001 to 0.005, see Abraham and Eysink, 1971), and α_{sr} = efficiency coefficient (ratio of roller length and wave length). The τ_{sr} -stress is applied for $H > H_{max}$ (breaking wave conditions). The roller effect may be important in the swash bar zone where plunging breaking waves are present.

The radiation force component is described by:

$$S_{xx} = (n - 0.5 + n \cos^2 \theta) E \quad (9)$$

Eq. (8) is solved for each wave height class. Each s -value is multiplied by the percentage of occurrence of the corresponding wave height class and the final representative s -value is obtained by summation over all classes. It may be argued whether this approach is valid because the set-up/set-down effect may not respond on the scale of individual waves.

Comparison of measured and computed results show however reasonably good agreement. Another (better) approach may be the application of the rms-wave height to determine the S_{xx} -values and hence the s -value from Eq. (8) in an iterative procedure.

2.4. Wave-induced longshore current

The depth-averaged longshore current related to breaking waves can be derived from the depth-averaged momentum equation for the longshore direction. Including wind-induced shear stress at the water surface and the (tide and wind-induced) longshore water surface gradient, the momentum equation reads, as:

$$\frac{\partial S_{xy}}{\partial x} + \rho g(h+s) \frac{\partial(h+s)}{\partial y} - \tau_{s,y} + \tau_{b,y} - \frac{\partial(h\tau_{xy})}{\partial x} = 0 \quad (10)$$

in which S_{xy} = radiation force in longshore direction; $\tau_{s,y}$ = shear stress at water surface due to longshore wind; $\tau_{b,y}$ = shear stress at bottom due to longshore current; τ_{xy} =

depth-averaged shear stress at side plane of water column; x = cross-shore coordinate (positive in onshore direction), y = longshore coordinate (positive in northward direction).

The gradient of the radiation force can be modelled (Fredsoe and Deigaard, 1992) as:

$$\frac{\partial S_{xy}}{\partial x} = - \frac{D_{br} \sin \theta}{c} \quad (11)$$

in which D_{br} = wave energy dissipation due to breaking, see Eq. (6); c = wave propagation velocity; θ = angle between wave propagation direction and shore normal.

Eq. (11) represents a local approach, which means that the wave-induced longshore velocity is related to the local value of the wave energy dissipation. It may be argued whether this is a realistic representation of the physics involved. It may take some distance (say 0.5 to 1 wave length) before the momentum of the breaking waves is fully transferred into momentum associated with the longshore current (through the roller mechanism), which can be seen as a relaxation or memory effect (transition zone). The relaxation effect of the roller mechanism in the transition zone on the computed longshore velocities will be studied in this paper.

The wind-induced shear stress is modelled, as:

$$\tau_{s,y} = \rho_a f_a w_{10} |w_{10,y}| \quad (12)$$

in which ρ_a = density of air ($= 1.25 \text{ kg/m}^3$); f_a = friction coefficient ($= 0.001$); $w_{10,y}$ = wind velocity component in the y -direction.

The bed-shear stress is modelled as:

$$\tau_{b,y} = \rho f_c v |v| \quad (13)$$

in which $f_c = g/C^2$ = current-related friction coefficient, $C = 18 \log(12h/k_a)$ = Chezy-coefficient; k_a = apparent bed roughness height; v = depth-averaged longshore current (in y -direction).

In this approach the effect of the near-bed wave motion on the near-bed current velocities is taken into account by use of the apparent bed roughness height (k_a) resulting in an increase of the physical current-related bed roughness (for example generated by the bed ripples). It has been shown that in a time-averaged approach the resulting bed-shear stress can be obtained by summation of the wave-related and the current-related bed-shear stresses, provided that the effect of the waves on the current velocity is taken into account (Van Rijn, 1993).

The apparent bed roughness is modelled, as (Van Rijn, 1993):

$$k_s = k_{s,c} \exp \left[\xi \frac{\hat{U}_{b,w}}{v} \right] \quad \text{and} \quad k_{a,\max} = 10 k_{s,c} \quad (14)$$

in which $\xi = 0.8 + \phi - 0.3(\phi)^2$ = coefficient; ϕ = angle between current direction and wave propagation direction (in radians); $\phi \leq \pi$, else $\phi = 2\pi - \phi$; $k_{s,c}$ = physical current-related bed-roughness; $\hat{U}_{b,w}$ = peak value of orbital velocity at edge of wave boundary layer based on $H_{1/3}$ and $T_{1/3}$.

The longshore water surface gradient $\partial(h+s)/\partial y$ is incorporated in Eq. (10) to represent the longshore water surface gradients related to two-dimensional flow systems

(for example tide and wind-induced flow) The magnitude of the longshore surface gradient should be known a priori. Measured longshore depth-averaged velocities around peak tidal flow outside the surf zone (offshore boundary) may be used to estimate the longshore surface gradient, as follows based on the Chézy-law:

$$\frac{\partial(h+s)}{\partial y} = - \left[\frac{v_{\text{meas}}^2}{C^2(h+s)} \right]_{x=0} \quad (15)$$

with v_{meas} = measured longshore velocity.

The longshore water surface gradient may be assumed to be constant in cross-shore direction.

The last term of Eq. (10) representing the cross-shore exchange of momentum is modelled as a dispersion term, as follows:

$$\frac{\partial(h\tau_{xy})}{\partial x} = \rho(h+s)\epsilon \frac{\partial^2 v}{\partial x^2} \quad (16)$$

in which $\epsilon = \epsilon_o + \epsilon_{\text{bf}} + \epsilon_{\text{br}}$ = dispersion or mixing coefficient; ϵ_o = large scale mixing coefficient ($0.1\text{--}10 \text{ m}^2/\text{s}$); $\epsilon_{\text{bf}} = 0.1u_*(h+s)$ = bottom-related mixing coefficient; $\epsilon_{\text{br}} = 0.025(h+s)(D_{\text{br}}/\rho)^{1/3}$ = breaking-related mixing coefficient; $u_* = (g^{0.5}/C)v$ = bed-shear velocity.

Eq. (10) is solved by using wave distribution-averaged variables. The D_{br} -parameter is represented as $D_{\text{br}} = \sum p_i D_{\text{br},i}$ with p_i = percentage of occurrence of wave height class i and $D_{\text{br},i}$ = local wave energy dissipation for wave height class i . Similarly, $\theta = \sum p_i \theta_i$ and $c = \sum p_i c_i$. The current refraction effect (Doppler shifting) is not taken into account at the present stage of research. This can, however, simply be realised by a loop over the computation procedure, if necessary.

Using Eqs. (11), (15) and (16), Eq. (10) can be rewritten as:

$$v|v| = \frac{C^2}{\rho g} \tau_{s,y} + \frac{C^2}{\rho g} \frac{D_{\text{br}}}{c} \sin \theta - C^2(h+s) \frac{\partial(h+s)}{\partial y} + \frac{C^2}{g}(h+s)\epsilon \frac{\partial^2 v}{\partial x^2} \quad (17)$$

Disregarding the dispersion term, Eq. (17) can be solved in a straightforward manner. The full equation is solved iteratively.

3. Calibration

The value of the friction coefficient (f_w), the breaking coefficient (γ) and the dissipation coefficient (α) were determined in a calibration procedure, aimed at giving the best overall agreement between measured and computed values of wave height, set-up and fraction of breaking waves. Regarding the wave height, the attention was focused on the higher waves represented by the significant wave height ($H_{1/3}$).

A constant friction coefficient (f_w) as well as a constant bed roughness height ($k_{s,w}$), see Eq. (4), have been used in the present computations. A constant $k_{s,w}$ -value implies

the application of a larger friction coefficient in Eq. (3) for smaller wave height classes. The surface shear stress τ_{sf} in Eq. (8) was set to zero for all tests.

The experimental data used for calibration were obtained from four tests (1A, 1C, 2A and 2B) carried out in 1993 in the Delta flume of Delft Hydraulics (Arcilla et al., 1994).

The Delta flume is a large flume of the following dimensions: length = 200 m, width = 5 m and depth = 7 m. The bed consisted of fine to medium coarse sand ($d_{50} = 200 \mu\text{m}$ and $d_{90} = 400 \mu\text{m}$). Before and after each test the bed levels were measured in three longitudinal sections. Irregular waves (Jonswap-spectrum) were generated. The wave board driving system was operated to minimize the reflection of long waves in the flume. Water level variations were measured by pressure sensors and by a resistance type wave gauge at various locations in the flume.

The instantaneous data were analyzed to determine the statistical parameters (wave heights H_{rms} , $H_{1/3}$, H_{mo} and set-up/set-down). For some tests the fraction of breaking waves was determined by analyzing video camera recordings. Each wave showing air entrainment (foam) at the measurement location was defined as a breaking or broken wave.

The wave data at the seaward boundary were schematized into 15 wave height classes and corresponding periods to run the WAVIS-model.

In all tests the friction coefficient was taken to be $f_w = 0.01$. The α_2 -coefficient giving the best agreement between measured and computed wave heights (focusing on $H_{1/3}$) was found to be $\alpha_2 = 1.5$, which is somewhat larger than the value reported by Battjes and Stive (1985). This is logical because in the present model the energy dissipation is related to $H^2 - H_{max}^2$, whereas H^2 was used by Battjes and Stive.

The γ -coefficient was found to be the most important calibration coefficient. The curve shown in Fig. 1, yields the best agreement between measured and computed values.

Fig. 2 shows measured and computed results for test 2A.

All parameters show good agreement between measured and computed values with the exception of the H_{rms} -values in the shallow surf zone which are overestimated by about 20%, see Fig. 2.

All calibration results are described in detail by Van Rijn and Wijnberg (1994).

Summarizing the results of four calibration tests, the $H_{1/3}$ -values are reasonably well represented in all zones from deep water to the shallow surf zone. The H_{rms} -values are overestimated in the shallow surf zone similar to those in Fig. 2. The cause for the systematic overestimation of the smaller wave heights is not yet clear but it may be related to the generation of smaller waves in the breaking process with a transfer of energy from the primary waves to the higher harmonics. It may also be related to the generation of low-frequency waves in the shallow surfzone. Waves with periods of 10 to 20 s were dominant in the shallow surf zone during some tests. Further study is necessary.

In the other calibration tests the set-up values are somewhat overestimated in the shallow surf zone near the water line, which may also be related to the overestimation of the wave heights.

The fraction of breaking waves is reasonably well represented by the model in conditions with a monotonically upsloping bed profile.

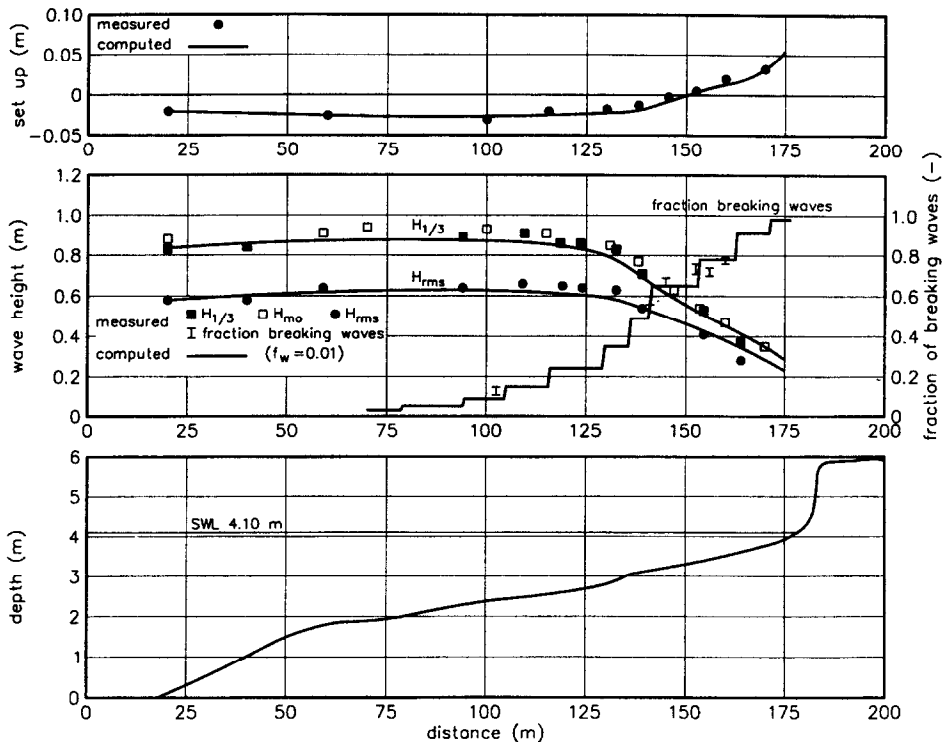


Fig. 2. Bed profile, wave heights, fraction of breaking waves and mean water level variations for Test 2A.

The calibration coefficients were systematically varied to analyze the effects on the computed results. The γ -coefficient was found to be the most sensitive parameter. A 10%-increase of the γ -coefficient results in an increase (maximum 15%) of the wave height and a considerable reduction of the fraction of breaking waves. A 10%-decrease of the γ -coefficient yields an increase of the fraction of breaking waves and a decrease of the wave height (maximum 15%). The α_2 -coefficient was varied in the range of 0.5 to 2.5. The standard value is $\alpha_2 = 1.5$. An increase from $\alpha_2 = 1.5$ to 2.5 yields a maximum decrease of 10% of the significant wave height in the shallow surf zone. A decrease from $\alpha_2 = 1.5$ to 1.0 results in a maximum increase of 10% of the wave height. The fraction of breaking waves is hardly affected by variation of the α_2 -coefficient.

The friction coefficient was increased from $f_w = 0.01$ to $f_w = 0.03$ resulting in a maximum decrease of 5% of the wave height.

The γ -coefficient is related to the ratio of the local bed slope and wave steepness, see Fig. 1. The bed slope is determined as the average value over a distance equal to half a wave length ($\beta = 0.5$) seaward of the local x -coordinate. This distance was varied from 0.25 to 1 wave length ($\beta = 0.25$ to $\beta = 1$). The β -coefficient has almost no effect on the model results in case of the presence of a monotonically upward sloping bed.

4. Verification of wave height and wave-induced set-up

Data from two other laboratory tests and nine field tests were used to verify the wave propagation model results of wave height, set-up and fraction of breaking waves (see Van Rijn and Wijnberg, 1994). One laboratory and four field experiments are presented in this paper. The model coefficients were set to the values obtained in the calibration procedure ($\alpha_2 = 1.5$, $\beta = 0.5$, γ according to Fig. 1). The computed wave set-up cannot be verified rigorously with the field data of mean water levels because both wave-induced and wind-induced effects are included. Another problem is the relatively large inaccuracy of the measured mean water levels. In the present field verification tests the τ_{sf} -value ($\tau_{sf} = \tau_{wind} + \tau_{sr}$) is set to zero, because data to estimate the wind shear stress τ_{wind} were lacking, as well as data to estimate τ_{sr} .

4.1. Laboratory verification

Two tests with irregular waves (single peaked spectrum) were carried out in a laboratory flume of the Delft University of Technology (Grasmeijer and Sies, 1994). The waves were propagating over a shallow sand bar followed by a deep trough, as shown in Fig. 3. The bed consisted of fine sand ($d_{50} = 100 \mu\text{m}$, $d_{90} = 130 \mu\text{m}$). Small scale ripples (height = 0.01 m, length = 0.07 m) were present at all locations in both tests. Based on this, the $k_{s,w}$ -value was considered to be 0.01 m.

Fig. 3 shows the results for Test B2. The discrepancy between computed and measured wave heights is of the order of 5%, which is quite good. The fraction of breaking waves is quite well predicted in the upsloping zone of the sand bar, but largely underestimated in the trough zone. This latter behaviour may be related to the definition of breaking waves adopted by the observers. At each location a breaking or broken wave was counted when a roller with foam was observed. Intensive breaking was observed at and right after the top of the bar. The major part of the roller generated near the wave crest decayed rapidly, but the foamy remains of the roller were carried by the wave crest over a distance of about 2 wave lengths (up to $x = 18$ m). It is questionable whether a very small roller with some foam on it (being the last remains of a broken wave) should be taken into account as much as a full breaking wave at the same location. The roller process is not simulated by the model; a breaking wave is defined to be present if $H > H_{\max}$.

4.2. Field verification

Generally, the offshore wave characteristics are available as spectral estimates, viz. H_{m0} and f_{peak} . An input wave field is constructed by assuming a Rayleigh distribution for the wave heights, i.e. $P(H > H^*) = \exp[-(H^*/H_{m0})^2]$. The H^* -parameter represents the boundary of an arbitrarily defined wave height class ($H_{m0} = H_{m0}/\sqrt{2}$).

Each wave class is represented in the model by the central value of the respective wave height classes. The wave period related to each wave height class is calculated by: $T = 5H^{0.5}$ (see Van Rijn, 1990). This simple schematization ignores the natural variation in wave period that occurs for a given wave height. In addition, it ignores that for

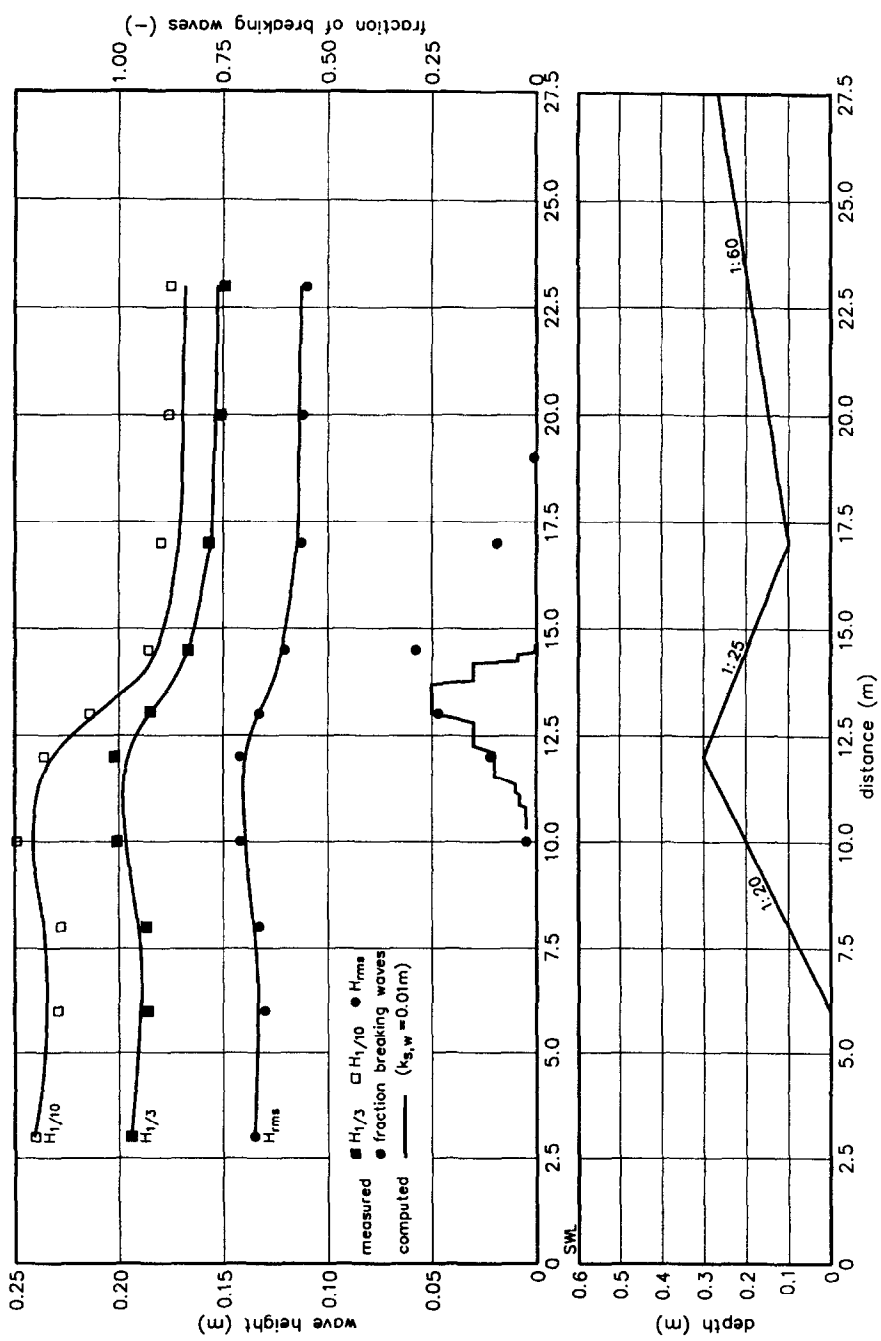


Fig. 3. Bed profile, wave heights and fraction of breaking waves for Test B2.

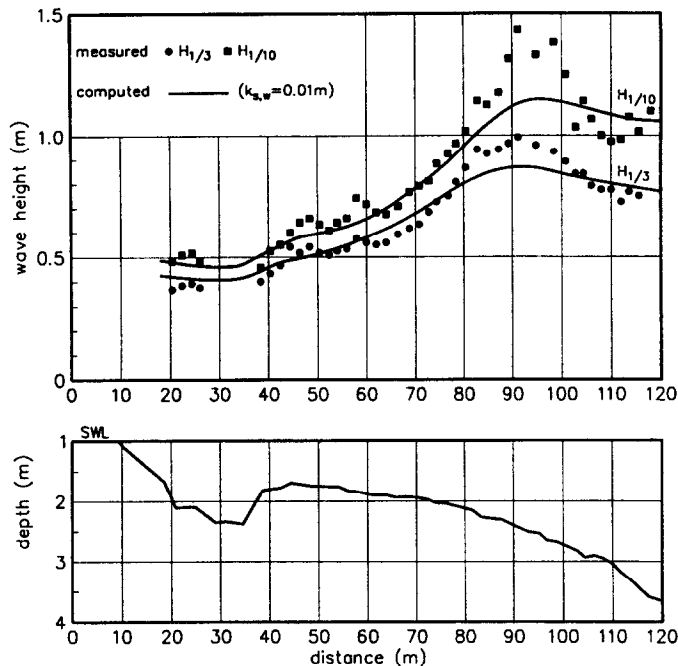


Fig. 4. Bed profile and wave heights, Ajigaura Beach, 1978, Japan.

the highest waves in the wave field the correlation between wave period and wave height becomes negligible (Goda, 1978; Longuet-Higgins, 1983). Nevertheless, given other uncertainties in the model, the less precise description of the wave field was considered acceptable at the present stage of research. The simple schematization appears to work rather well. A more precise representation of the wave field is simply possible by using more classes of wave height–wave period. Similarly, the wave field may be represented in more detail by taking into account the directional spreading of the wave field.

4.2.1. Ajigaura beach, 1978, Japan

Field measurements were carried out in 1978 at Ajigaura beach facing the Pacific Ocean located at the southern end of Tokai coast about 200 km from Tokyo. The average tidal range is about 1.2 m. The beach slope is about 1 to 60. The bed consists of sand in the range of 200 to 500 μm (Hotta and Mizuguchi, 1980). A breaker bar was present in the surf zone, see Fig. 4.

In the nearshore zone about sixty poles were placed in the bed at intervals of about 2 m normal to the shore over a total distance of 120 m. The most seaward pole was outside the surf zone (surf zone width of about 80 m). The significant wave height at this latter pole was about 0.7 m (periods of 6 to 11 s) during the test conditions (July 5, 1978). The water surface elevations along the poles were photographed from a pier situated parallel (50 m northward) to the pole line.

Fig. 4 shows measured and computed wave heights. The computed wave heights using a roughness height of $k_{s,w} = 0.01$ m are about 20% too small in the zone between $x = 80$ m and $x = 100$ m. The reason for this discrepancy is not quite clear. It may be related to reflection phenomena because cross-shore undulations can be observed in the wave height statistics at various locations. Another cause may be the use of linear wave theory which leads to an underestimation of the wave height of shoaling waves, especially for relatively low long-period waves (swell type waves). Kamphuis (1994) obtained better agreement between computed and measured $H_{1/3}$ -wave heights by using nonlinear shoaling for this test case.

4.2.2. Duck beach 1985, USA

A photopole experiment (Dally, 1992) was conducted on September 4–6, 1985 at the Field Research Facility of the U.S. Army Coastal Engineering Research Center (CERC) in Duck, North Carolina. The photopole method is described in detail by Hotta and Mizuguchi (1980). Fourteen poles at intervals of 6 to 7 m were placed in the surf and swash zone. The most seaward pole was outside the zone of breaking waves.

The waves approaching the shore can be characterized as long-crested swell (periods of 10 to 12 s) with a majority of plunging breakers. The tidal range was about 0.5 m. The significant wave height at the most seaward pole varied between 0.4 and 1 m during

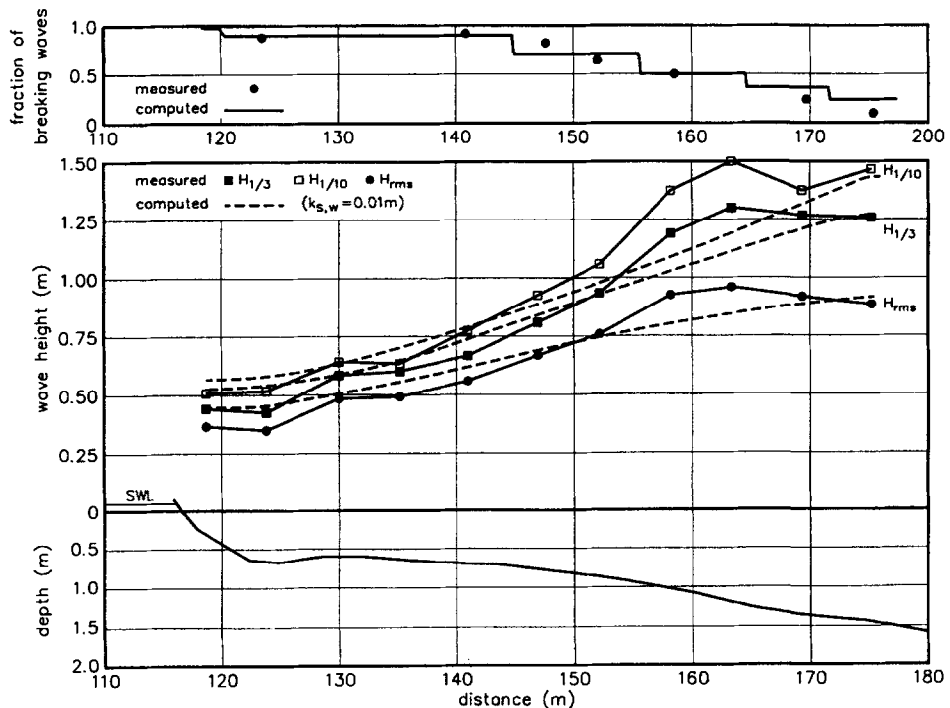


Fig. 5. Bed profile, wave heights and fraction of breaking waves, Duck Beach 1985, USA.

the tests. A steady offshore wind (6 to 7 m/s) was present during the tests. Test 41510 (Sept. 4, 15.10 hrs) is herein used for validation. During this test the incoming wave energy was maximum, the rms-wave height attained a value of 1 m at pole 11. All waves had broken before reaching pole 5, while 11% had reformed at pole 4. Pole 3 was in the swash zone during this test. Wind effects were visually observed to have a noticeable influence on the breaking process. According to Dally, offshore wind delays breaking resulting in larger wave heights closer to the shore. Reflected waves were also observed to exist at various poles. For example, cross-shore undulations in the wave statistics ($H_{1/3}$, $H_{1/10}$) can be observed at poles 4, 10 and 11, see Fig. 5.

Measured and computed wave heights and the fraction of breaking waves are shown in Fig. 5. The computed wave heights are significantly too small in the zone between $x = 155$ m and $x = 165$ m and too large in the zone near the waterline. The discrepancies may be caused by reflection phenomena which are not represented in the model. Another cause for discrepancies is the use of linear wave theory which leads to

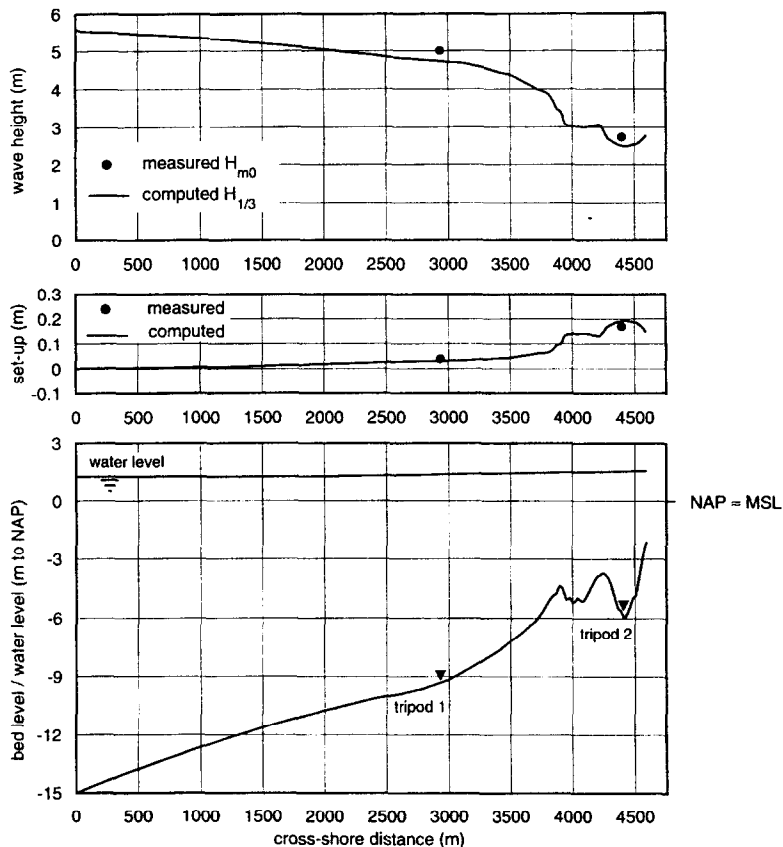


Fig. 6. Bed profile, wave height and mean water level variations, Terschelling case 1, 11 November 1993, Netherlands.

underprediction of the wave height of shoaling waves, especially for low long-period (swell type) waves as present in the Duck area during the tests. Similar findings were reported by Kamphuis (1994).

The fraction of breaking waves is reasonably well predicted between 120 and 160 m, see Fig. 5.

4.2.3. Terschelling case 1, 11 November 1993, Netherlands

The wave data were measured by use of a wave buoy in the offshore zone and by pressure gauges attached to tripods in the nearshore zone (Ruessink, 1994). The offshore wave height H_{m0} during the storm of November 11 (22.00 hrs) 1993 was as large as 5.5 m in a water depth of 16.25 m. The waves were approaching the shore in a normal direction ($\theta = 0^\circ$). The measured wind set-up in cross-shore direction was taken into account. The bed consists of fine to medium coarse sand with diameters in the range of 200 to 500 μm . Major breaker bars were present in the surf zone. A constant friction coefficient of $f_w = 0.01$ was used. Fig. 6 shows the bed profile, wave height $H_{1/3}$ and wave set-up.

The model predictions of $H_{1/3}$ are very satisfying. Especially the accurate prediction of $H_{1/3}$ in the trough is very satisfying, because a considerable fraction of the wave field has been breaking seaward of this location. In the offshore zone the $H_{1/3}$ value is smaller than the H_{m0} value ($H_{1/3} = 0.95 H_{m0}$; see Horikawa, 1988). In the surf zone the $H_{1/3}$ value is generally found to be larger than the H_{m0} value (Horikawa, 1988). This implies that the value of $H_{1/3}$ is predicted reasonably well near tripod 1 but is underpredicted near tripod 2.

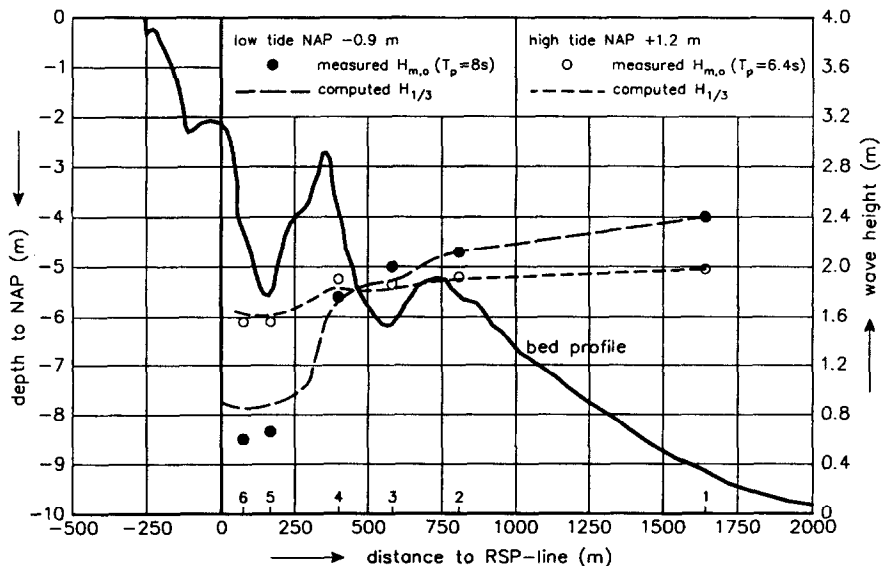


Fig. 7. Bed profile and wave height, Terschelling case 2, 10 June 1994, Netherlands.

The agreement between measured and predicted wave-induced set-up in the shallow surf zone is quite good.

4.2.4. Terschelling case 2, 10 June 1994, Netherlands

Time series of water pressures using instrumented poles and tripods were measured in a cross-shore profile at the North Sea coast of the barrier island of Terschelling (Ruessink, 1994). The bed profile is shown in Fig. 7. Major breaker bars can be observed. The wave direction during the storm on June 10 was normal to the shore ($\theta = 0^\circ$). The pressure data were converted to wave height data using linear wave theory. Fig. 7 shows H_{mo} -wave heights for two tidal conditions: high tide (burst 5314) and low tide (burst 5321). At low tide the majority of the waves break at the middle bar (350 m from RSP-line) resulting in a large decrease of the wave height in the trough landward of the bar crest (stations 5 and 6). The computed $H_{1/3}$ -wave heights based on Rayleigh-distributed waves in Station 1 and a constant bed roughness of $k_{s,w} = 0.01$ m are shown in Fig. 7.

Good agreement between measured and computed results can be observed at high tide. At low tide the computed values in the deep trough region landward of the middle bar are much too large (30%). Better agreement (not shown) was obtained by using a γ -coefficient of 0.35 instead of 0.45 for $\tan\beta/(H/L) = 0$ (see Fig. 1). These values are applied in the trough region with negative bed slopes (negative bed slopes on the landward side of the bar are set to zero). Further research of the energy decay in the trough region between bars is necessary.

5. Verification of wave-induced longshore current

Data from three field experiments were used to verify the computation of the depth-averaged wave-induced longshore velocities. The coefficients were set to the values obtained in the calibration procedure of the wave propagation model ($\alpha_2 = 1.5$, $\beta = 0.5$, γ according to Fig. 1).

5.1. Lake Michigan beach, 1978, USA

Measurements from a towed, instrumented sled were used to determine the cross-shore distribution of wave heights and longshore currents across the surf zone on a steep, barred beach on Lake Michigan during two storms (Allender and Ditmars, 1981). Deep-water wave information was obtained from a wave-rider buoy. Local wave data were obtained from resistance-wire wave staffs placed on a line normal to the shore in depths of 0.5, 0.8, 1.5 and 2.5 m. The sled was equipped with a wave staff and two bidirectional ducted-impeller current meters placed at 0.5 m and 1 m above the bottom of the sled. The signals of the current meters were averaged over about 5 wave periods. Two storm experiments were conducted. Data from the second experiment on April 29–30, 1978 are used herein for verification. During each data-collection cycle (about

45 min) the sled was moved from offshore to the beach. At each measurement location 5-minute records of waves and currents were obtained. The bed profile (average of pre and post-storm values), the H_{rms} -wave heights and the longshore current velocities (3 cycles) are shown in Fig. 8. The longshore wind-component was of the order of 10 m/s. Deep water wave approach was very oblique with breaking angles of about 25 to 30°. The wind-induced water level rise at the shoreline was about 0.25 m. Breaker heights (H_{rms}) varied in the range of 0.8 to 1 m. The longshore currents reached magnitudes of about 1.7 m/s. The differences between the current velocities measured at 0.5 m and 1.0 m above the bed were found to be small.

In the beginning of the storm (cycle 1) the longshore current velocity shows a rather peaked distribution. In later cycles (5 and 9) a relatively uniform velocity distribution was found in the trough zone between the bar crest and the shoreline, see Fig. 8B. This latter effect may be caused by: (i) non-local momentum transfer from breaking waves to the longshore current (lag effect), (ii) horizontal (cross-shore) mixing and (iii) by longshore gradients in wave set-up related to variations in breaker type (spilling and plunging breakers) and longshore bar variability.

Neglecting horizontal mixing ($\epsilon = 0 \text{ m}^2/\text{s}$), the computed velocity distribution is very peaked with maximum velocities of about 1.6 m/s near the bar crest, where most of the waves are breaking (see Fig. 8B). In the trough zone and in the zone seaward of the bar crest the computed velocities are of the order of 0.2 m/s as a result of wind-induced shear-stresses. Fig. 8B also shows computed velocities for mixing coefficients of 0.5 and 1 m^2/s , which are typical values for a cross-shore length scale of 100 m (Van Rijn, 1990). Using these values, more uniform velocity distributions are obtained. The computed velocities in the trough zone (about 0.5 m/s) are, however, much too small compared to the measured values.

Fig. 8C shows the effect of a longshore water surface gradient on the computed velocity distribution based on sensitivity computations. A constant longshore water surface gradient was imposed in the trough zone ($x < 100 \text{ m}$). The value of the longshore surface gradient was determined by trial and error until good agreement with measured velocities was obtained. As shown in Fig. 8C, a mixing coefficient of $\epsilon = 0.5 \text{ m}^2/\text{s}$ and a longshore water surface gradient of $dh/dy = -0.001$ yields computed velocities of the right order of magnitude (1 m/s) in the trough zone. A longshore water surface gradient of $dh/dy = -0.001$ means a drop in mean water level of 0.1 m over a longshore distance of 100 m. As the maximum computed wave set-up near the shoreline is about 0.05 m, this means that the longshore variation of the set-up should be about 0.05 m over 50 m and remain constant over some time to generate a steady current. Field measurements of longshore current velocities should include set-up measurements in longshore transects to determine whether water surface gradients of the order of 0.001 are realistic. Further research is necessary.

Fig. 8D shows computed longshore velocities based on two different methods to represent the dissipation term (D_{br} , see Eq. (17)) related to the breaking waves: (1) the local value of the dissipation term and (2) the space-averaged (over one wave length seaward of local coordinate) value of the dissipation term. This latter method results in a landward shift of the velocity distribution, which is in better agreement with the measured velocities.

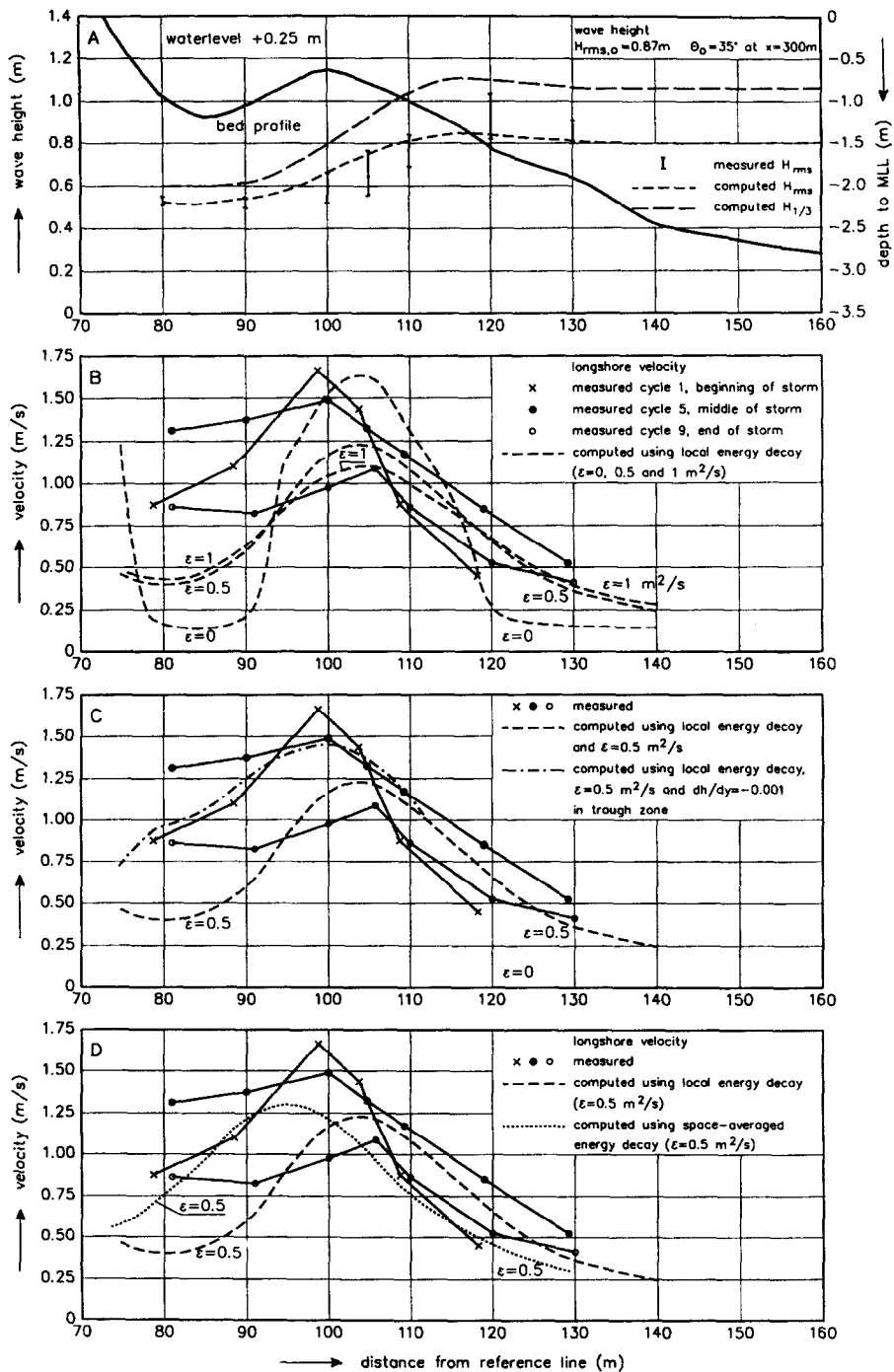


Fig. 8. Bed profile, wave heights and longshore velocity, Lake Michigan, 1978, USA.

5.2. Santa Barbara beach, 1980, USA

The data used herein were measured on February 4, 1980 at Leadbetter beach, Santa Barbara, California, USA as part of the Nearshore Sediment Transport Study (NSTS), (Thornton and Guza, 1986). The beach is composed of well-sorted fine to medium size sand. The mean nearshore slope varied between 0.03 and 0.06. No major offshore bar was apparent. The winds were generally light during the measurement period. The incident waves were almost entirely derived from the deep ocean resulting in a narrow band swell ($H_{rms} = 0.56$ m, $T_p = 14$ s and $\theta = 9^\circ$ at a depth of 3.8 m about 90 m from the shoreline). Plunging breakers were most often observed in the surf zone. Wave

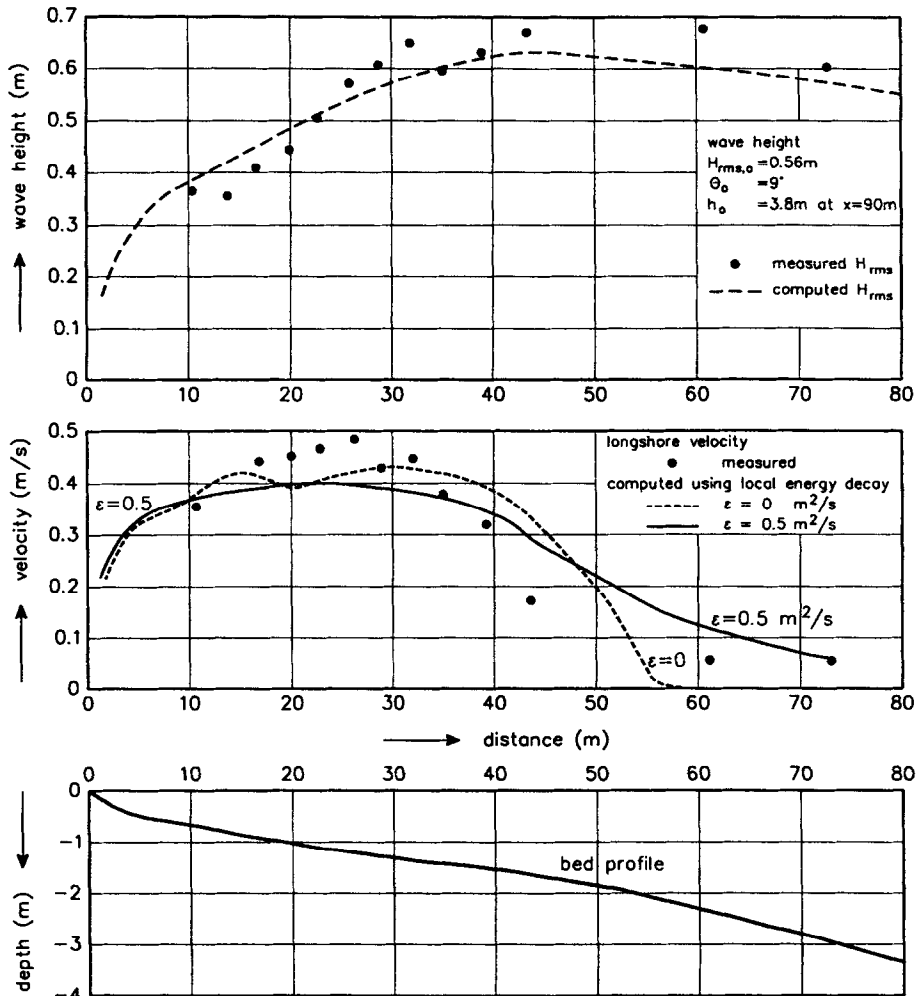


Fig. 9. Bed profile, wave height and longshore velocity, Santa Barbara beach, 1980, USA.

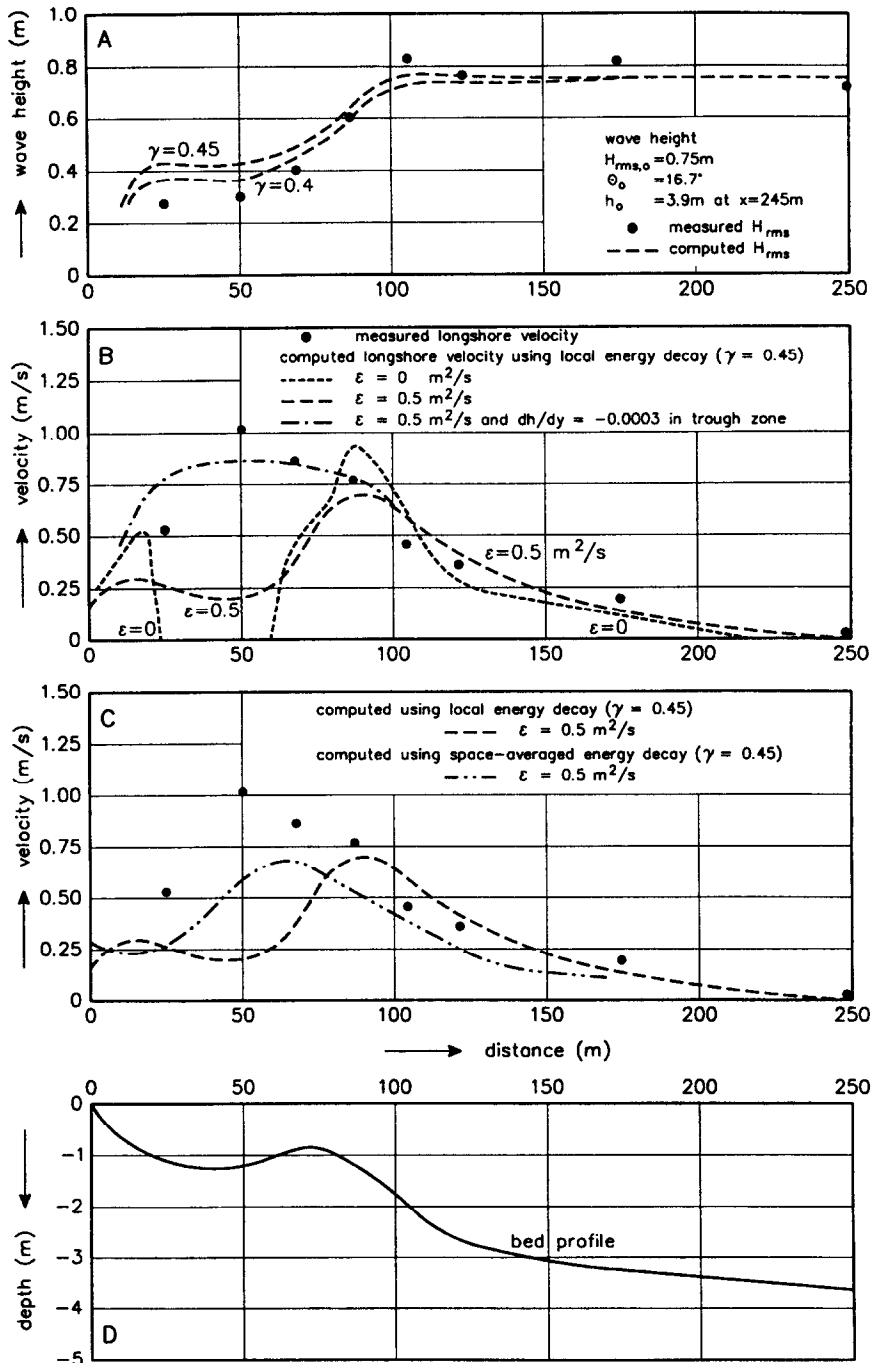


Fig. 10. Bed profile, wave heights and longshore velocity, Duck beach, 1990, USA.

height data were derived from pressure sensors; velocity data were derived from electromagnetic current meters. All instruments were simultaneously deployed. The data are shown in Fig. 9. Computed results are also shown in Fig. 9. The wind velocity was set to zero. The bed roughness was taken as $k_{s,w} = 0.01$ m. The use of a breaking coefficient according to Fig. 1 did not give an optimum prediction of the wave height distribution in the surf zone and hence the breaking-related energy dissipation, which is of crucial importance for the breaking-induced longshore current. Therefore, the breaking coefficient was adjusted for this specific case. A constant breaking coefficient of $\gamma = 0.45$ was found to give reasonable agreement between measured and computed H_{rms} -wave height. The applied breaking coefficient of $\gamma = 0.45$ is rather small. Based on Fig. 1, the breaking coefficient should be of the order of 0.8 for the present case with low-steepness waves. The reason for this discrepancy is not yet clear. Further research related to the breaking of narrow band swell waves is required.

Longshore depth-averaged velocities were computed for $\epsilon = 0$ and $0.5 \text{ m}^2/\text{s}$. Reasonable agreement between measured and computed values can be observed for $x < 35$ m. Just outside this zone the computed velocities are considerably larger than the measured values. This may be related to inaccurate representation (Rayleigh-type distribution was assumed) of the wave height distribution of the incoming swell. No information was given by Thornton and Guza (1986). Using a non-local representation of the energy dissipation, somewhat smaller longshore velocities were obtained (not shown).

5.3. Duck beach, 1990, USA

The field data were measured on October 10, 1990 at Duck beach, North Carolina, USA as part of the Delilah-experiment (Church and Thornton, 1992). A relatively small bar was present at a distance of about 75 m from the shoreline. The incident waves were arriving from 17° and the peak wave frequency was 0.094 Hz ($T_p \approx 11 \text{ s}$). All available data are shown in Fig. 10. Computed results are also shown in Fig. 10. The wind velocity was set to zero. The bed roughness was taken as $k_{s,w} = 0.01$ m. A constant breaking coefficient of $\gamma = 0.45$ was used similar to the Santa Barbara experiment. A constant breaking coefficient of $\gamma = 0.4$ yields somewhat better result.

Longshore depth-averaged velocities were computed for $\gamma = 0.45$, $\epsilon = 0$ and $0.5 \text{ m}^2/\text{s}$, using a local and a space-averaged wave energy dissipation (see Fig. 10B and C). Reasonable agreement between measured and computed velocities can be observed for $x > 100$ m (outside the surf zone). The use of a breaking coefficient of $\gamma = 0.4$ hardly influences the computed longshore velocities (not shown). Imposing a longshore water surface gradient of $dh/dy = -0.0003$ for $x < 75$ m, yields computed velocities of the right order of magnitude (Fig. 10B). This longshore water surface gradient of -0.0003 means a drop in mean water level of 0.03 m over a longshore distance of 100 m. It is unknown whether this is a realistic assumption for this specific case. However, Reniers and Thornton (1995) indicate that the longshore pressure gradient may play a dominant role in the surf zone depending on the longshore variability of the bathymetry at the Duck site. Further research is necessary.

Fig. 10C shows that space-averaging of the breaking-related energy dissipation term yields better results than a local approach. The computed velocities in the trough zone are much too small, using the local energy decay method.

6. Discussion and conclusion

Generally, the measured $H_{1/3}$ -wave heights in the calibration tests are reasonably well represented by the probabilistic model in all zones from deep water to the shallow surf zone. The H_{rms} -values are generally overestimated in the shallow surfzone, which may be related to the generation of smaller waves in the breaking process with a transfer of energy from the primary waves to the higher harmonics. The wave-induced set-up values are somewhat overestimated in the zone near the mean water line.

Comparison of the computed wave heights with laboratory data (waves over breaker bar in flume) shows good agreement for the H_{rms} , $H_{1/3}$ and $H_{1/10}$ wave parameters. The fraction of breaking waves is reasonably well described in the upsloping zone of the breaker bar. In the trough zone of the bar the fraction of breaking waves is significantly underestimated by the model. This may, however, be related to the definition of breaking and broken waves in the experiments, which is primarily based on the observation of a roller with foam near the wave crest. It may be argued whether a small roller with some foam should be taken into account as much as a full breaking wave at the same location.

Verification of the computed wave heights with wave data from various coastal areas shows somewhat inconsistent results. In some cases the agreement between measured and computed values is reasonably good. In other cases the wave heights in the surf zone are under or overestimated. The wave heights in the deep trough region between two breaker bars seem to be overestimated (Terschelling case 2, 1994). Further research is necessary. Relatively small breaking coefficients of about 0.45 were found for two cases with low-steepness swell-type waves (Santa Barbara, 1980 and Duck, 1990). Based on Fig. 1, the breaking coefficient should be of the order of 0.8. The reason for this discrepancy is unknown. Further research related to the breaking of narrow band swell waves is necessary.

In the Duck beach case and the Ajigaura beach case non-linear shoaling is required to obtain optimum agreement between measured and computed $H_{1/3}$ - and $H_{1/10}$ -wave heights as pointed out by Dally (1992) and Kamphuis (1994). In most other cases good results were obtained by using linear shoaling. At the present state of research it is not clear when to use linear or nonlinear shoaling.

Verification of the model results with respect to wave-induced longshore current velocities was not extensive, because of a lack of data. In case of a barred profile the measured longshore velocities showed a relatively uniform distribution in the (trough) zone between the bar crest and the shoreline, which could to some extent be modelled by including space-averaging of the energy dissipation, horizontal mixing and longshore water surface gradients related to variations in set-up. Further research is necessary. In case of a monotonically sloping profile (Santa Barbara, USA) the cross-shore distribution of the longshore current velocities is reasonably well represented, except for a small zone just outside the breaker region where the velocities are overestimated by a factor 2. This may be related to inaccurate representation of the wave height distribution of the incoming swell; no data of this distribution were available.

The importance of the surface shear stresses related to the breaking roller effect should be studied in more detail, especially in strongly plunging breaking waves (swash

bar zone). This may improve the computed wave-induced set-up and hence the wave height in the shallow surf zone. Field experiments in the outer and inner surf zone especially designed for verification purposes are necessary to obtain detailed and accurate information of wave heights, wave-induced set-up, fraction of breaking waves and especially the mean wave-induced longshore currents. In this way some of the inconsistencies discovered in the field verification results may be solved.

Acknowledgements

The verification of the model for field conditions required accurate field data. This data was generously supplied by various people. We would like to thank B.G. Ruessink (Utrecht University, Netherlands) for supplying data for the Terschelling case (Nourtec Program). F.C.J. Wolf (Utrecht University, The Netherlands) is thanked for providing the field data for the Egmond cases (Coastal Genesis Program). E.B. Thornton (Naval Postgraduate School, USA) is thanked for supplying field data for the Santa Barbara case and the Duck case (Delilah experiment). J.A. Roelvink and A. Reniers of Delft Hydraulics are gratefully acknowledged for many stimulating discussions on wave propagation modelling.

References

- Abraham, G. and Eysink, W., 1971. Magnitude of interfacial shear in exchange flow. *J. Hydraul. Res.*, 9(2): 125–153.
- Allender, J.H. and Ditmars, J.D., 1981. Measurements of longshore currents on a barred beach. *Coastal Eng.*, 5: 295–309.
- Arcilla, A.S., Roelvink, J.A., O'Connor, B.A., Reniers, A. and Jimenez, J.A., 1994. The Delta Flume 1993 Experiment. In: *Proceedings Coastal Dynamics 1994, Barcelona*, pp. 488–502.
- Battjes, J.A. and Janssen, J.P.F.M., 1978. Energy loss and set-up due to breaking of random waves. In: *Proc. 16th Int. Coastal Engineering Conf., Hamburg*, pp. 569–587.
- Battjes, J.A. and Stive, M.J.F., 1985. Calibration and verification of a dissipation model for random breaking waves. *J. Geophys. Res.*, 90(C5): 9159–9167.
- Church, J.C. and Thornton, E.B., 1992. Bottom stress modification by breaking waves within a longshore current model. In: *Proc. Int. Coastal Eng. Conf., Venice*.
- Dally, W.R., 1992. Random breaking waves: field verification of a wave-by-wave algorithm for engineering application. *Coastal Eng.*, 16: 369–397.
- Dally, W.R., Dean, R.G. and Dalrymple, R.A., 1985. Wave height variation across beaches of arbitrary profile. *J. Geophys. Res.*, 90(C6): 11917–11927.
- Dally, W.R. and Dean, R.G., 1986. Transformation of random breaking waves on surf beat. In: *Proc. 20th Int. Coastal Engineering Conf., Taipei, Vol. 1*, pp. 109–123.
- Fredsøe, J. and Deigaard, R., 1992. *Mechanics of Coastal Sediment Transport*. World Scientific, Singapore.
- Goda, Y., 1978. The observed joint distribution of periods and heights of sea waves. In: *Proc. 16th Int. Conf. Coastal Engineering, Hamburg*, pp. 227–246.
- Grasmeijer, B.T. and Sies, E.M., 1994. Sand Concentrations and Transport in Breaking Wave Conditions. Delft Univ. of Technology, Coastal Eng. Dep., Delft.
- Horikawa, K. and Kuo, C.T., 1966. A study on wave transformation inside surf zone. In: *Proc. Int. Coastal Engineering Conf., Tokyo, Vol. 1*.
- Horikawa, K. (Editor), 1988. *Nearshore Dynamics and Coastal Processes. Theory, Measurement and Predictive Models*. University of Tokyo Press, 522 pp.

- Hotta, S. and Mizuguchi, M., 1980. A field study of waves in the surf zone. *Coastal Eng. Jpn.*, 23: 59–81.
- Kamphuis, J.W., 1994. Wave height from deep water through breaking zone. *J. Waterw. Port Coastal Ocean Eng. ASCE*, 120(4): 347–368.
- Kroon, A., 1994. Sediment transport and morphodynamics of the beach and nearshore zone near Egmond, The Netherlands. Doctoral Thesis, Dep. of Physical Geography, University of Utrecht, The Netherlands.
- Le Méhauté, B., 1962. On non-saturated breakers and the wave run-up. In: *Proc. 8th Int. Coastal Engineering Conf.*, Mexico City, pp. 1178–1191.
- Longuet-Higgins, M.S., 1983. On the joint distribution of wave periods and amplitudes in a random wave field. *Proc. R. London Ser. A*, 389: 241–258.
- Mase, H. and Iwagaki, Y., 1982. Wave height distributions and wave grouping in surf zone. In: *Proc. 18th Int. Coastal Engineering Conf.*, Cape Town, pp. 58–76.
- Mizuguchi, M., 1982. Individual wave analysis of irregular wave deformation in the nearshore zone. In: *Proc. 18th Int. Coastal Engineering Conf.*, Cape Town, pp. 485–504.
- Nelson, R.C., 1983. Wave heights in depth-limited conditions. In: *Sixth Australian Conf. on Coastal and Ocean Engineering*, Gold Coast (Australia).
- Putnam, J.A. and Johnson, J.W., 1949. The dissipation of wave energy by bottom friction. *EOS (Trans. AGU)*, 30: 67–74.
- Reniers, A. and Thornton, E.B., 1995. Longshore currents over barred beaches. In: *Coastal Dynamics*, Gdansk.
- Roelvink, J.A., 1993. Dissipation in random wave groups incident on a beach. *Coastal Eng.*, 19: 127–150.
- Ruessink, G., 1994. Overview of process measurement campaign, spring 1994, Nourtec Terschelling. Note, Dep. of Phys. Geography, Univ. of Utrecht.
- Sato, S., Ozaki, M. and Shibayama, T., 1990. Breaking conditions of composite and random waves. *Coastal Eng. Jpn.*, 33(2): 133–145.
- Shuto, N., 1974. Non-linear long waves in a channel of variable section. *Coastal Eng. Jpn.*, 17: 1–12.
- Southgate, H.N. and Naim, R.B., 1993. Deterministic profile modelling of nearshore processes. Part 1, Waves and currents. *Coastal Eng.*, 19: 27–56.
- Stive, M.J.F. and Dingemans, M.W., 1984. Calibration and verification of a one-dimensional wave-energy decay model. Report M 1882, Delft Hydraulics, Delft.
- Thornton, E.B. and Guza, R.T., 1983. Transformation of wave height distribution. *J. Geophys. Res.*, 88: 5925–5938.
- Thornton, E.B. and Guza, R.T., 1986. Surf zone longshore currents and random waves: field data and models. *J. Phys. Oceanogr.*, 16: 1165–1178.
- Van Rijn, L.C., 1990. *Principles of Fluid Flow and Surface Waves in Rivers, Estuaries, Seas and Oceans*. Aqua Publications, Amsterdam.
- Van Rijn, L.C., 1993. *Principles of Sediment Transport in Rivers, Estuaries and Coastal Seas*. Aqua Publications, Amsterdam.
- Van Rijn, L.C. and Wijnberg, K.M., 1994. One-dimensional modelling of individual waves and wave-induced longshore currents in the surf zone. Report R 94-09, Dept. of Physical Geography, Univ. of Utrecht.
- Weggel, J.R., 1972. Maximum breaker height. *J. Waterw. Harbors Coastal Eng. Div. ASCE*, 98(WW4): 529–549.
- Wolf, F.C.J., 1993. Data reports of field experiment Egmond aan Zee, The Netherlands. Dep. of Physical Geography, Univ. of Utrecht, The Netherlands.